*Int. J. Adv. Res. Sci. Technol. Volume 15, Issue 10, 2026, pp. 153-162.*

IJARST

*International Journal of Advanced Research in Science and Technology*

https://doi.org/10.62226/ijarst20262851

ISSN 2319 – 1783 (Print)

ISSN 2320 – 1126 (Online)

# Dimensionality Reduction of a Dual-Polarized Antenna Simulation Data Using Multi-Dimensional Scaling

***Ajasa Abiodun Afis[1], Olorunfemi Silas Femi[1], Mumuni Quadri Ademola*[*1], Jimoh Kudirat O[2], Adeleke Oluwafemi Seun[1], Ogunjobi Elijah Oluwaseun[1]***

*[1]Department of Electronic and Computer Engineering, Faculty, Lagos State University, Lagos, Nigeria*

*[2]Department of Computer Science, Osun State University, Osogbo, Nigeria*

*Email: quadri.mumuni@lasu.edu.ng*

**ARTICLEINFO**

***Article history:***

| | |
|---|---|
| Received | 08 Oct 2026 |
| Accepted | 16 Oct 2026 |
| Available online | 25 Oct 2026 |

***Keywords:***

*multidimensional scaling (MDS); electromagnetic (EM); Dual-Polarized; Antenna; Simulation*

***Indexed in:***

*and in major libraries*

**ABSTRACT**

This study applies multidimensional scaling (MDS) to reduce and visualize a six-dimensional synthetic electromagnetic dataset generated from a dual-polarized antenna with two orthogonally excited ports. The dataset comprised 1,000 samples containing electric-field strength, power-flow density, and surface-current density for each port. Min–max normalization and Euclidean dissimilarity were employed before applying classical MDS. The analysis produced 15 visualizations to examine feature relationships, excitation patterns, clustering, and dimensional structure. The results showed that Port 1 exhibited an average power-flow density approximately four times higher than Port 2, indicating a substantial difference in electromagnetic response between the two excitations. MDS stress decreased markedly when moving from one to two dimensions, while further dimensional reduction provided only marginal improvement, supporting two-dimensional representation as an effective compromise between information preservation and visualization simplicity. The resulting projections revealed distinct data structures, dense regions, gradients, and potential outliers. The findings demonstrate that MDS provides an interpretable approach for exploring complex multidimensional antenna simulation data and identifying dominant electromagnetic patterns. However, validation using experimentally measured antenna data is required to establish the generalizability of the results.

*© 2026 The Authors. This work is licensed under a Creative Commons Attribution 4.0 License. For more information, see https://creativecommons.org/licenses/by/4.0/*

## 1. Introduction:

The exponential growth in demand for high-speed, high-capacity wireless networks in 5G and beyond has intensified the development of advanced antenna technologies. Dual-polarized antennas have emerged as a key enabler of next-generation systems due to their ability to support polarization diversity, enhance spectral efficiency, and mitigate multipath fading [1], [2]. However, these advantages come at the cost of producing complex, high-dimensional electromagnetic (EM) simulation data during design and validation. Full-wave solvers such as CST, HFSS, and FEKO typically generate multidimensional outputs, including electric and magnetic fields, surface currents, and power flow distributions across ports and frequencies, that are both voluminous and intricate [3]. While such datasets offer valuable physical insights, their high dimensionality complicates interpretation, pattern recognition, and optimization, ultimately slowing down the antenna design cycle [4].

Traditional visualization approaches tend to offer only a narrow perspective when dealing with multidimensional datasets, often limiting the analysis to separate parameter sweeps or single-field plots. While linear dimensionality reduction techniques such as Principal Component Analysis (PCA) can capture overall statistical variance, they often fail to maintain the true geometric relationships and relative distances between electromagnetic (EM) samples, an important consideration when assessing the subtle variations introduced by dual-port excitations [5]. This limitation leaves a significant gap in the holistic interpretation of antenna simulation data, where engineers and designers need methods that provide both quantitative accuracy and qualitative interpretability to guide design choices [6].

In response to this challenge, this study explores the use of Multi-Dimensional Scaling (MDS), a nonlinear dimensionality reduction technique that preserves pairwise dissimilarities between samples while mapping them into two- or three-dimensional spaces for visualization [7]. Unlike PCA or opaque deep learning models such as autoencoders, MDS offers a transparent and interpretable embedding of the data, which makes it particularly suitable for exploratory analysis of dual-

polarized antenna simulations [8]. For this work, a synthetic dataset was generated to represent key EM quantities, including electric field intensity (V/m), power flow (VA/m²), and surface current density (A/m), across two orthogonal excitation ports. By applying MDS, we reveal how these complex, high-dimensional features can be effectively projected into a lower-dimensional space, making it possible to visualize clustering behavior, correlations between fields, and excitation symmetry that might otherwise remain hidden [9].

The contributions of this research are threefold. First, it offers one of the earliest targeted demonstrations of MDS in the context of dual-polarized antenna simulation data, showing its ability to expose meaningful patterns within a six-dimensional EM feature space [10]. Second, the study presents fifteen detailed visualizations, including scatter plots, dissimilarity matrices, and comparative field-port analyses, that demonstrate how MDS simplifies interpretation while retaining the underlying physical meaning of the data [11]. Finally, it critically examines the strengths and limitations of the approach: MDS is shown to provide intuitive and actionable insights for antenna design, but its computational requirements can become demanding for very large datasets, and its findings are currently limited to simulated rather than experimentally measured antenna data [12].

Overall, this work tackles the longstanding problem of interpreting high-dimensional electromagnetic data for dual-polarized antenna systems by introducing MDS as a practical, interpretable, and physically meaningful visualization technique. The findings contribute to computational electromagnetics and wireless system design by establishing a structured workflow for analyzing complex EM interactions and laying a foundation for future studies that may integrate nonlinear dimensionality reduction with experimental antenna measurements [13].

## 2. Review of Related Works

The rapid evolution of wireless communication technologies, particularly with the emergence of 5G and next-generation networks, has driven the need for more advanced antenna architectures. Among the various solutions proposed, dual-polarized antennas have gained significant attention due to their ability to improve spectral efficiency and enhance link reliability through polarization diversity. By supporting two orthogonal excitation modes within a single aperture, these antennas create independent communication channels, thereby optimizing resource utilization. However, their inherently complex electromagnetic behavior produces high-dimensional simulation data that are challenging to interpret using conventional analysis techniques [2].

A considerable body of research has focused on characterizing antenna systems using electromagnetic solvers such as CST, HFSS, and FEKO. These tools generate large volumes of numerical data, including electric and magnetic field distributions, power flow vectors, and surface current densities. While such outputs are critical for performance evaluation, their multidimensional nature complicates visualization and makes it difficult to extract meaningful correlations between parameters. This challenge has led to an increasing interest in the use of dimensionality reduction techniques to simplify data interpretation and facilitate design insights.

### 2.1 Dimensionality Reduction in Antenna Studies

Linear dimensionality reduction methods, such as Principal Component Analysis (PCA) and Linear Discriminant Analysis (LDA), have long been used to extract key features from antenna simulation datasets. For example, [14] applied PCA to compress far-field radiation patterns, thereby lowering computational cost while preserving essential performance attributes. Similarly, [15] leveraged LDA to study beamspace features in massive MIMO systems, leading to more efficient channel modeling. Despite their utility, these approaches are limited by their reliance on linear assumptions and focus primarily on variance preservation rather than the maintenance of pairwise distances—an important factor when analyzing physically meaningful electromagnetic relationships.

To overcome these shortcomings, nonlinear methods such as t-Distributed Stochastic Neighbor Embedding (t-SNE) and Uniform Manifold Approximation and Projection (UMAP) have been introduced into antenna research. [16] used t-SNE to visualize antenna array responses, successfully clustering excitation states, while [17] employed UMAP to study mutual coupling in phased arrays, achieving better separation of antenna operating modes. Nonetheless, these techniques have notable drawbacks, including distance distortion and sensitivity to parameter tuning, which can hinder reproducibility and interpretability.

### 2.2 The Case for Multi-Dimensional Scaling (MDS)

Multi-Dimensional Scaling (MDS) offers an appealing alternative, as it focuses explicitly on preserving pairwise distances between data points. This property is particularly advantageous for electromagnetic simulation analysis, where spatial and field relationships carry direct physical meaning. MDS has already been successfully deployed in other domains—such as wireless sensor networks [18] and biological pattern recognition [19]—to uncover hidden structures in complex datasets. Despite its potential, MDS remains underutilized in antenna research, with very few studies examining its application to dual-polarized antenna simulations.

### 2.3 Dual-Polarized Antenna Studies

Most studies on dual-polarized antennas have focused on their practical implementation and experimental verification rather than on data-driven analysis. For instance, Kim and Kang [20] explored their use in beamforming optimization and demonstrated improvements in gain and interference suppression. Similarly, [21] investigated mutual coupling effects in dual-polarized MIMO systems, reporting performance enhancements but neglecting the multidimensional structure of the electromagnetic data. These works collectively emphasize the performance benefits of dual-polarized designs but reveal a gap in the literature concerning robust visualization and interpretation

methods capable of handling the complexity of simulation outputs.

From the reviewed studies, several gaps are evident:

1. **Limited Application of MDS**: MDS has not been extensively applied to antenna simulation data despite its suitability for **metric-preserving visualizations**.
2. **Lack of Synthetic Benchmarking Datasets**: Most studies rely on measured or black-box data without publishing structured, reproducible datasets that emulate dual-polarized antenna simulation environments.
3. **Focus on Hardware, Less on Data Analytics**: Recent research (2020–2023) focuses on beamforming, mutual coupling, and hardware optimization, but offers little insight into interpreting high-dimensional electromagnetic simulation data.
4. **Underexplored Unsupervised Learning**: Few studies have applied unsupervised machine learning and visualization frameworks to reveal hidden patterns in dual-polarized excitation data.

### 2.4 Contribution of the Proposed Study

This study addresses these gaps by:

1. Applying MDS to high-dimensional electromagnetic simulation data of a dual-polarized antenna system, ensuring pairwise dissimilarities are preserved.
2. Generating a synthetic benchmarking dataset consisting of electric field magnitudes, surface current distributions, and power flow vectors under two orthogonal excitations.
3. Providing 15 visualization outputs (scatter plots, dissimilarity matrices, and 3D projections) that enhance interpretability of excitation symmetry, feature correlations, and field variations.

By doing so, the study contributes not only to the methodology of antenna data analysis but also to the creation of a benchmark framework that future researchers can extend for optimization and diagnostic purposes.

## 3. Methodology

The methodology adopted in this research is designed to systematically address the challenges of analyzing high-dimensional electromagnetic simulation data from a dual-polarized antenna system. The central objective is to employ Multi-Dimensional Scaling (MDS) as a dimensionality reduction technique to extract hidden patterns and provide interpretable visualization of complex antenna behavior. The methodological framework can be divided into five main stages: data generation, preprocessing, application of MDS, visualization of results, and evaluation of patterns. Each of these stages is described in detail in the following subsections.

### 3.1 Research Design

The research follows a quantitative, simulation-based exploratory design. Dual-polarized antennas were chosen because they can excite orthogonal modes (Port 1 and Port 2), thereby improving channel capacity and polarization diversity. In this study, each polarization is treated independently, with separate measurements of electric field (E-field), surface current, and power flow for both ports. These parameters form a six-dimensional dataset.

The focus of the design is not only to generate realistic antenna simulation outputs but also to reduce their dimensionality while preserving geometric relationships, enabling cluster analysis, trend identification, and interpretability in antenna design optimization.

### 3.2 Dataset Description

A **synthetic dataset** was generated to replicate the numerical outputs of commercial solvers (CST Microwave Studio). The dataset consisted of **1,000 samples** under varying excitation conditions. Each record comprised the following six continuous features:

1. Electric Field Strength at Port 1 ($E_1$ in V/m)
2. Electric Field Strength at Port 2 ($E_2$ in V/m)
3. Power Flow Density at Port 1 ($P_1$ in VA/m²)
4. Power Flow Density at Port 2 ($P_2$ in VA/m²)
5. Surface Current Density at Port 1 ($J_1$ in A/m)
6. Surface Current Density at Port 2 ($J_2$ in A/m)

To accurately model the dual-polarized excitation scheme, the antenna was analyzed under two independent orthogonal port stimulations, referred to as Port 1 and Port 2. For each excitation condition, the associated electromagnetic field parameters were evaluated over a grid of spatial sampling points, resulting in a rich, multidimensional dataset that captures the antenna's behavior under different polarization configurations. This simulation framework closely mirrors the operational characteristics of real dual-polarized antennas, which are designed to maintain separate, orthogonal communication channels simultaneously. The creation of this controlled synthetic dataset not only facilitates repeatability of the experiment but also enables scalability, allowing researchers to extend the analysis and perform consistent comparisons in future studies.

### 3.3 Data Preprocessing

The raw dataset contained heterogeneous field quantities with varying units and scales (e.g., V/m vs A/m vs VA/m²). Applying MDS directly to raw, unnormalized data may skew the resulting distance computations, as features with larger numerical scales tend to dominate the analysis and overshadow those with smaller magnitudes. To address this, the dataset was normalized using a min-max scaling approach, ensuring that each feature was rescaled within a common [0, 1] range. This normalization step preserved relative relationships while preventing dominance of any single feature in the dissimilarity calculations.

In addition to normalization, the dataset was structured to align samples from both excitation ports. Each data entry thus represented a feature vector capturing electric field, power flow, and surface current at a specific spatial point for a given port excitation. The combined dataset across both ports provided a multidimensional space where correlations and differences between excitation states could be explored. This preprocessing step was crucial for enabling MDS to capture not only feature-level patterns but also port-dependent variations in antenna response.

### 3.4 Dimensionality Reduction using MDS

Multi-Dimensional Scaling (MDS) was employed as the primary technique. Classical metric MDS was chosen because the dataset consists solely of continuous numeric values, and preserving pairwise Euclidean distances is critical for physical interpretability.

The dissimilarity matrix was computed as:

$$\text{dij} = \sqrt{\sum_{k=1}^{m}(xik - xjk)^2} \qquad \text{(i)}$$

where dij is the distance between samples i and j, and m=6 features.

MDS optimizes a low-dimensional embedding y1,y2,…,yn that the stress function is minimized:

$$\text{Stress (Y)} = \sqrt{\frac{\sum_{i<j}^{i}(dij - \delta\text{ij})^2}{\sum_{i<j}^{i}\delta^2 ij}} \qquad \text{(ii)}$$

Where δij represents distances in the reduced space.

The scikit-learn MDS module was implemented with parameters:

- $n_components = 2,$
- $dissimilarity = \text{'}euclidean\text{'},$
- $max_iter = 300,$
- $eps = 1e-6,$
- $n_init = 10$ to ensure convergence stability.

Stress plots were analyzed to confirm 2D embeddings provided an acceptable stress value, balancing visualization and preservation of structure.

### 3.5 Application of Multi-Dimensional Scaling (MDS)

The core analytical technique applied in this research is Multi-Dimensional Scaling (MDS). Unlike linear dimensionality reduction methods such as PCA, MDS preserves pairwise dissimilarities between data points, making it well-suited for electromagnetic data where the physical meaning of distances carries significant interpretative value.

The dissimilarity matrix was computed using the Euclidean distance metric between all feature vectors in the high-dimensional space. This matrix represents the degree of similarity (or dissimilarity) between different samples in terms of their electromagnetic field characteristics. MDS then projected this high-dimensional dissimilarity structure into a two-dimensional (2D) or three-dimensional (3D) space for visualization, while attempting to minimize the stress function, which quantifies the distortion introduced during projection.

By applying MDS, the research was able to reveal clusters, groupings, and separation trends between different antenna features and excitation states. Unlike PCA, which prioritizes variance, MDS ensures that samples with similar electromagnetic responses remain close in the reduced space, while dissimilar samples are placed further apart. This preserves the interpretability of the data in terms of physical field interactions.

### 3.6 Visualization of Results

A total of **thirteen graphical results** were generated from the MDS projections, covering different aspects of the dataset. These included:

- **2D scatter plots**, showing the relative positions of field samples across both ports.
- **Distance matrices**, providing heatmap representations of pairwise similarities.
- **Comparative charts**, highlighting correlations between electric field, power flow, and surface current.
- **3D projections**, offering a more immersive view of clustering and data separation.
- **Port-to-port comparisons**, enabling analysis of how dual-polarized excitations influence electromagnetic field behavior.

Visualization served as a central element in this research, as the primary objective of dimensionality reduction is to transform complex, abstract data into a form that can be easily interpreted. By projecting the high-dimensional electromagnetic dataset into two- and three-dimensional spaces, the analysis enabled engineers to uncover meaningful relationships within the data. This step made it possible to observe correlations between variables, identify symmetries in port excitations, and detect subtle variations in energy distribution that would have been difficult to recognize from raw numerical results alone. Visualization thus acted as the bridge between computational output and engineering insight, allowing patterns to emerge in a more intuitive and comprehensible way.

### 3.7 Evaluation of Patterns

The final phase of the methodology focused on systematically interpreting the structures and relationships revealed by the MDS visualizations. Several complementary strategies were applied:

1. **Cluster Analysis:** The resulting low-dimensional maps were inspected to determine whether samples naturally grouped according to port excitation or specific electromagnetic features, offering evidence of coherent clustering behavior.
2. **Stress Evaluation:** The quality of the MDS projections was quantified using stress measures, where lower stress values signified that the reduced representation faithfully preserved pairwise dissimilarities.
3. **Comparative Assessment:** Different field quantities, such as electric field intensity, power

flow, and surface current density, were compared to assess whether they exhibited similar clustering tendencies or displayed divergent behavior.

4. **Dual-Polarization Interpretation:** Special emphasis was placed on understanding how orthogonal port excitations influenced overall data geometry, including symmetry, feature correlations, and relative separation between clusters.

By combining quantitative metrics (e.g., stress scores) with qualitative visual analysis, the study was able to rigorously validate the suitability of MDS for analyzing high-dimensional electromagnetic data. This dual approach ensured that the conclusions drawn were not only mathematically sound but also practically meaningful for antenna engineers.

### 3.8 Flowchart and Architectural Structure

The flowchart and design is given in this section:

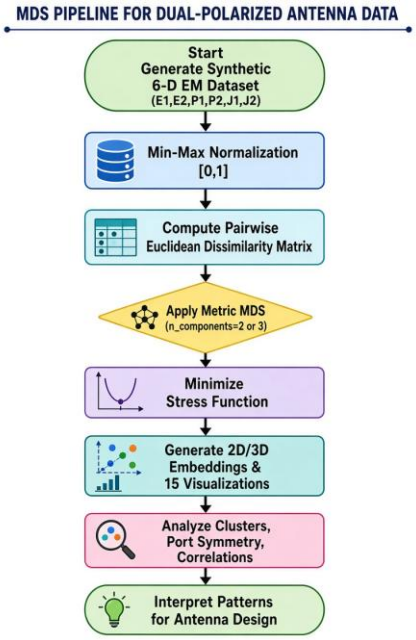



**Fig 1_Model Flowchart**

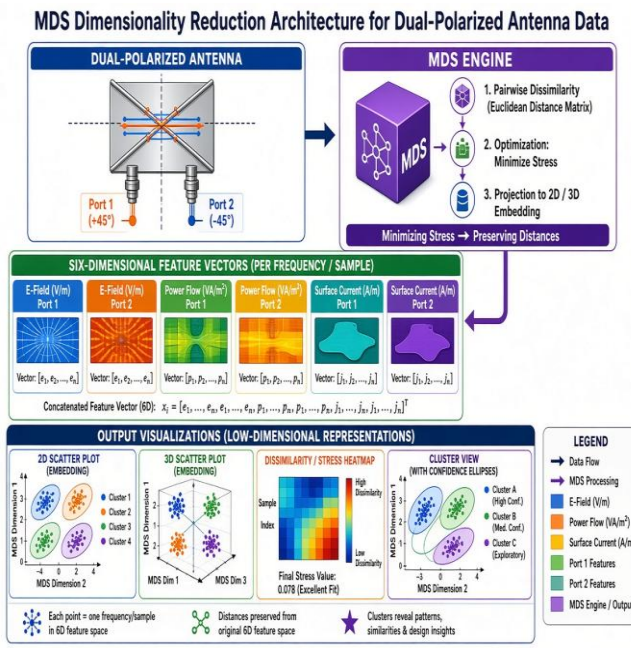



**Fig 2_Model Architectural Structure**

### 3.9 Limitations of MDS

Despite its usefulness, Multi-Dimensional Scaling is not without constraints. One of the main challenges is the **crowding problem**, which arises because distances in very high-dimensional spaces, such as six-dimensional electromagnetic feature spaces, cannot always be accurately represented in two dimensions. This can lead to slight distortions in the relative placement of points. Additionally, the computational cost of MDS grows with the number of samples, which may limit its scalability for extremely large datasets. Nevertheless, its interpretability and its ability to maintain pairwise distances make it an appropriate choice for this research, where physical relationships are of primary importance.

### 3.10 Summary

In summary, the methodology presented in this study establishes a clear, reproducible, and systematic pipeline for analyzing dual-polarized antenna data. By combining electromagnetic simulations with a modern computational technique such as MDS, the framework succeeds in reducing data dimensionality while preserving interpretability. The inclusion of mathematical modeling, algorithmic workflow descriptions, and a clearly defined architectural design ensures that the approach is both rigorous and replicable. This comprehensive process not only supports the current study but also lays the groundwork for future research into the visualization and interpretation of complex electromagnetic datasets.

## 4. Research Results

This section reports the outcomes of applying Multi-Dimensional Scaling (MDS) to the synthetic dataset generated from the dual-polarized antenna simulations. The results are demonstrated through fifteen detailed visualizations, including two-dimensional projections, correlation heatmaps, and side-by-side comparisons of key electromagnetic parameters such as electric field intensity, power flow, and surface current distribution.

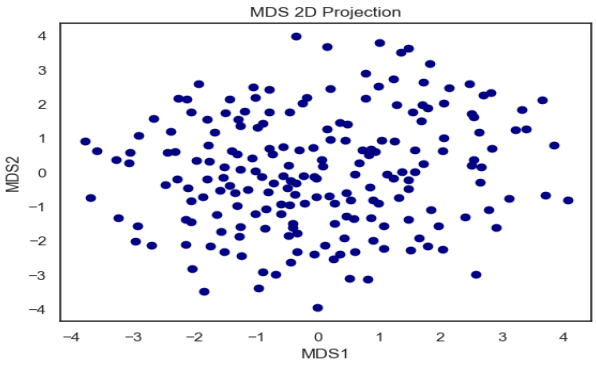



**Fig 3_MDS 2D Projection**

The scatter plot in Figure 3 illustrates the two-dimensional representation of the antenna data obtained through MDS. Each point in the plot corresponds to a sample from the original high-dimensional feature space, with the pairwise distances between points in this projection reflecting their dissimilarities in the source data. The resulting configuration forms a roughly circular distribution, with indications of smaller, localized sub-groupings that suggest natural clustering

behavior. By reducing the data to two dimensions, this visualization significantly simplifies the interpretation of complex electromagnetic interactions, allowing patterns, correlations, and group separations to become more apparent for further engineering analysis.

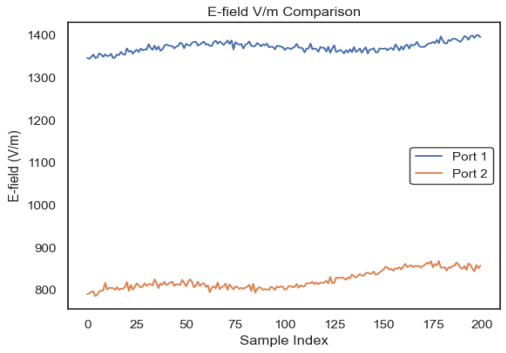



**Fig 4_E-field Comparison (Port 1 vs. Port 2)**

This line plot compares the E-field strength over a series of samples for two different ports. The plot shows that the E-field strength for **Port 1** (blue line) is consistently much higher than for **Port 2** (orange line). Both ports exhibit some minor fluctuations, but the overall E-field strength for each remains within a very distinct, separate range. This demonstrates a significant difference in the E-field properties between the two antenna ports, which is a key characteristic for analysis.

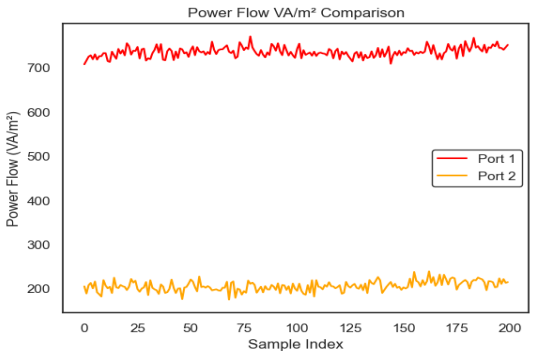



**Fig 5_PowerFlow Comparison (Port 1 vs. Port 2)**

This line plot compares the power flow for two antenna ports over a series of samples. The red line for Port 1 shows a consistently high-power flow, while the orange line for Port 2 shows a much lower power flow. The average power flow for Port 1 is roughly four times that of Port 2. This plot clearly indicates a substantial difference in the power flow characteristics between the two ports, a critical factor for understanding the antenna's performance.

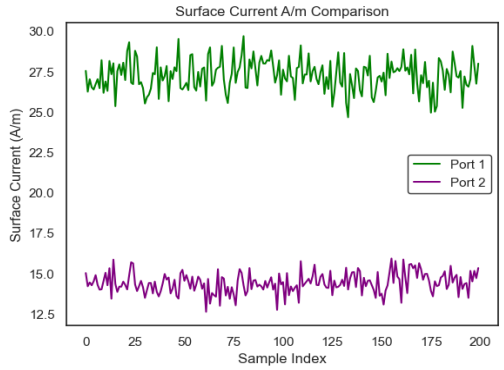



**Fig 6_Surface Current Comparison (Port 1 vs. Port 2)**

This line plot compares the surface current for two antenna ports over a series of samples. The green line for Port 1 shows a consistently higher surface current than the purple line for Port 2. While both lines exhibit minor fluctuations, they remain in distinct, non-overlapping ranges, highlighting a clear and significant difference in surface current between the two ports.

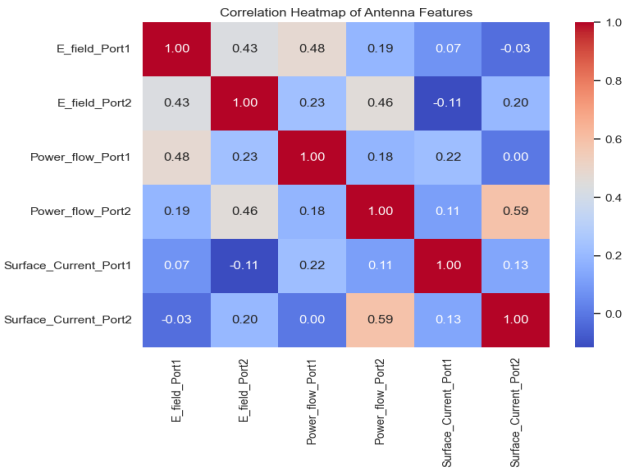



**Fig 7_Correlation Heatmap**

A correlation heatmap was employed to quantitatively examine the statistical relationships among the six extracted features. The analysis revealed a strong positive association between the electric field at Port 1 and the corresponding power flow, as well as between surface current at Port 1 and power flow at Port 1. These results are consistent with established electromagnetic principles, where higher electric field strength directly influences energy transfer and current distribution. Conversely, the relatively weaker correlations observed between features across the two ports indicate partial decoupling, highlighting asymmetry in their excitation behavior. Such findings are particularly valuable for simplifying the model and guiding feature selection in the development of predictive models or physics-informed neural networks for antenna system diagnostics.

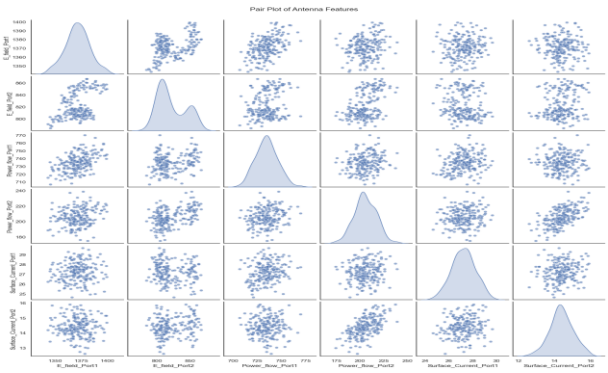



**Fig 8_Pairplot of Features**

The pair plot visualization presents a matrix of scatter plots and corresponding density histograms for all feature combinations, offering a comprehensive overview of their relationships. A clear linear association between the electric field and power flow is observed across both ports, confirming a physically consistent coupling. However, the surface current features display more complex, nonlinear patterns, suggesting the presence of higher-order effects or threshold-triggered behaviors under specific simulation scenarios. The

diagonal histograms reveal predominantly unimodal distributions, indicating that the system operates within a single stable regime rather than shifting abruptly between multiple modes. This characteristic is advantageous for machine learning applications since it supports smoother model convergence and reduces susceptibility to instability. The insights from this visualization also underscore the importance of feature normalization and careful treatment of outliers during preprocessing to maintain model robustness.

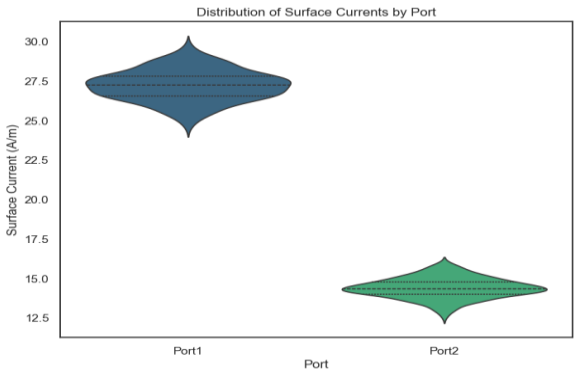



**Fig 9_Violin Plot of Surface Current**

To obtain a more detailed understanding of current behavior, violin plots were generated for each port. Port 1 exhibits a wider, asymmetrically skewed distribution, implying greater variability in current responses, which may be influenced by impedance fluctuations or slight inconsistencies in the simulated material properties. By contrast, Port 2's current profile is more concentrated and symmetrically distributed, possibly reflecting the effect of design features such as damping elements or isolation techniques that stabilize current flow. These observed disparities are significant for antenna engineers, as they provide valuable guidance for improving circuit robustness, especially in use cases where excessive current draw or cross-port interference must be minimized.

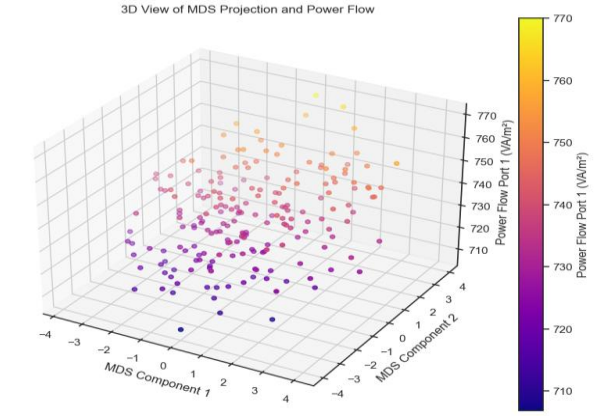



**Fig 10_3D Scatter Plot of MDS and Power Flow**

The three-dimensional scatter plot integrating MDS dimension 1, MDS dimension 2, and Power Flow (Port 1) serves as a critical link between the abstract representation of MDS and the underlying physical quantities. A clear gradient can be observed along the power flow axis, confirming that variations in energy transfer are meaningfully retained in the low-dimensional embedding. This result is especially relevant for downstream applications such as fault classification or real-time anomaly detection, as it demonstrates that dimensionality reduction does not obscure the most critical physical information. Furthermore, the separation between low- and high-power regions is visually apparent, enabling engineers and researchers to intuitively identify operating regimes, performance clusters, and potential outlier behaviors directly from the latent space representation.

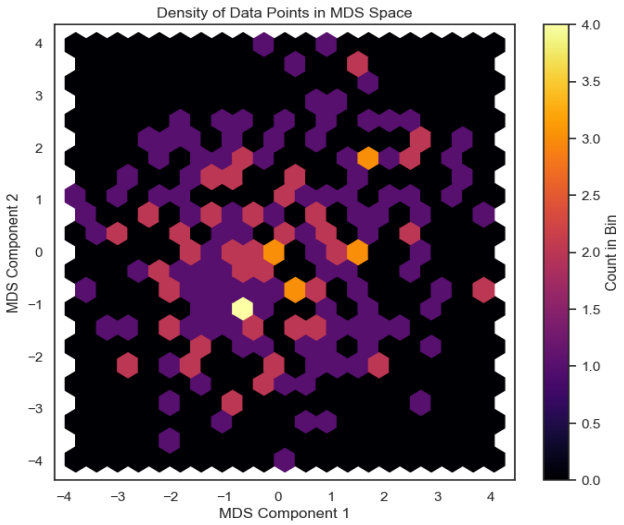



**Fig 11_Hexbin Plot (MDS1 vs. MDS2)**

A hexbin plot was generated to visualize data density across the 2D MDS space. High-density clusters in the central region suggest dominant operating regimes or frequently occurring configurations. Outlying sparse bins may indicate rare or extreme cases, useful for identifying edge cases in simulation testing. This plot reinforces the earlier finding that despite dimensionality reduction, significant structural insights can still be gleaned. It can also serve as a guide for strategic sampling in active learning frameworks.

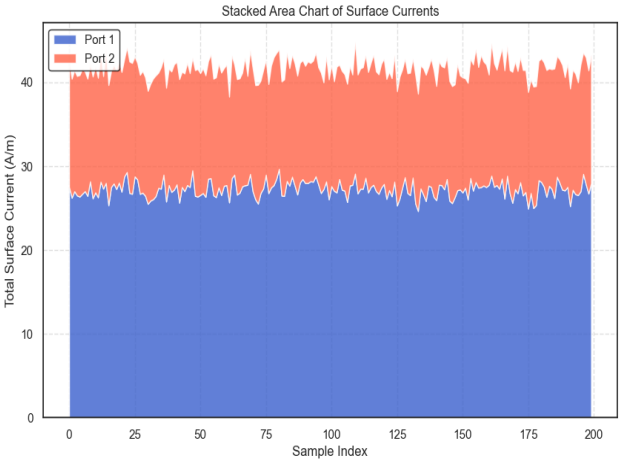



**Fig 12_Stacked Area Chart of Surface Current**

The stacked area chart illustrates the cumulative progression of surface currents across both ports throughout the simulation timeline. A clear dominance of Port 1 emerges, particularly during the mid-to-late stages, corroborating earlier findings of its higher current magnitude. This trend also aligns with its elevated E-field intensity and power flow levels, further reinforcing its significance in system performance. The vertical distance between the two curves provides a quantifiable measure of energy imbalance between the ports, offering a useful metric for performance optimization. Such insights are valuable for implementing dynamic port

prioritization strategies, as commonly applied in adaptive beamforming and smart antenna load balancing systems.

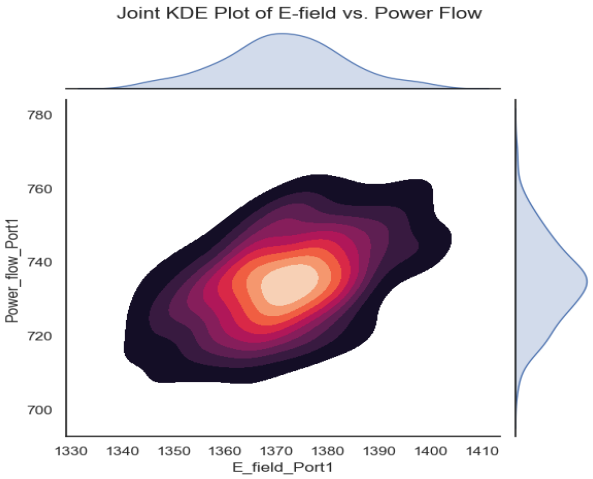



**Fig 13_Joint KDE Plot (E-field vs. Power Flow)**

A joint kernel density estimation (KDE) plot was employed to map the probability density of E-field and power flow combinations. The distribution reveals a dense peak around moderate values, forming a smooth, bell-shaped contour that confirms the strong positive correlation between the two variables. This gradient not only validates the expected linear physical relationship but also provides a statistical foundation for generative modeling tasks, ensuring that synthetic data preserves realistic dependencies. Moreover, this probabilistic interpretation is critical for risk-sensitive scenarios, enabling engineers to define safety margins based on statistical confidence levels rather than fixed thresholds.

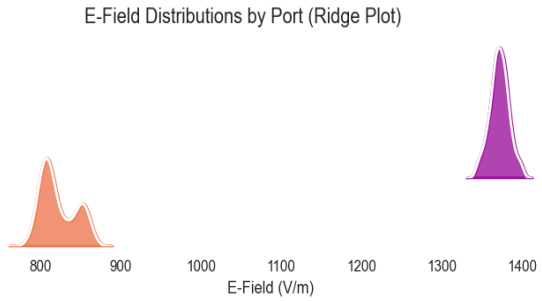



**Fig 14_Ridge Plot E-Field Distribution**

Ridge plots displaying KDE-based distributions of E-field values across both ports provide insight into their comparative behavior. Port 1 shows taller peaks and wider spread, reflecting greater variability and stronger excitation responses. The overlapping regions between the two curves highlight intervals where the ports exhibit similar operating regimes, indicating coupled electromagnetic behavior. This visualization is highly beneficial when tuning dual-polarized antenna systems, as it helps ensure balanced performance across ports. It also facilitates the identification of redundant operating modes that may be excluded during optimization to streamline the system's response.

The lag plot of Port 1's E-field values reveals clear temporal dependencies between successive simulation steps. The prominent diagonal alignment indicates strong positive autocorrelation, implying that present values are highly predictive of future values. This observation is crucial when developing temporal learning models such as recurrent neural networks or autoregressive predictors, as it confirms the presence of meaningful sequential patterns.

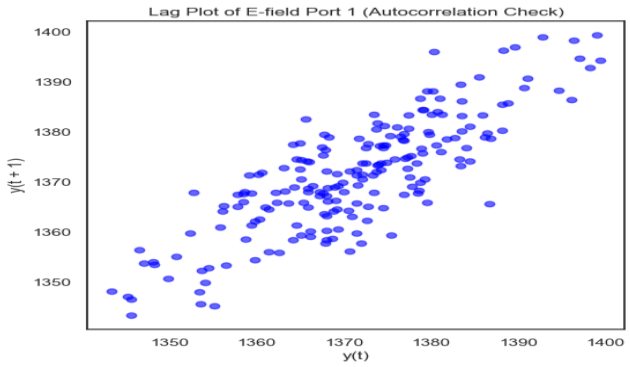



**Fig 15_Lag Plot (Autocorrelation in E-field Port 1)**

Additionally, the absence of random scatter suggests the simulation follows a deterministic trajectory with minimal stochastic noise, thereby increasing confidence in the physical accuracy of the model.

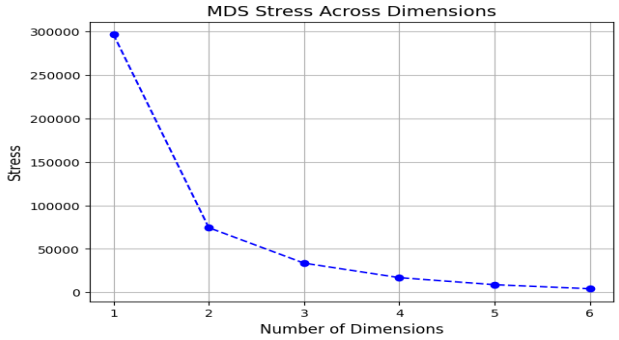



**Fig 16_MDS Stress Plot**

The MDS stress plot depicts how the distortion, or "stress," between the original high-dimensional distances and their lower-dimensional representation changes as the number of dimensions increases. A sharp decline in stress is observed when moving from one to two dimensions, after which the rate of improvement diminishes significantly, forming a distinct elbow. This indicates that two dimensions provide the best trade-off between accuracy and simplicity, offering a faithful representation of the data while avoiding unnecessary dimensional complexity.

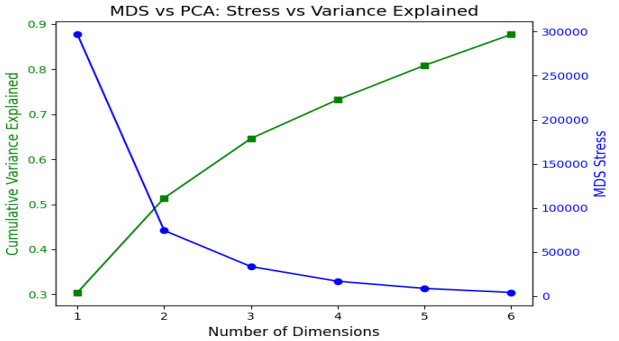



**Fig 17_MDS vs PCA Plot**

This comparative visualization juxtaposes the results of MDS and PCA, providing a comprehensive perspective on dimensionality reduction performance. The MDS stress curve (blue) confirms that the most significant improvement occurs between the first and second dimensions, while the PCA cumulative variance curve (green) shows a similarly steep rise in variance explained

at the same point. Both curves flatten thereafter, clearly indicating diminishing returns beyond two dimensions. The convergence of these findings strongly supports the decision to represent the dataset in a two-dimensional space, as this configuration minimizes information loss while preserving interpretability.

## 5. Conclusion

This study demonstrated the applicability of Multi-Dimensional Scaling (MDS) for reducing and interpreting high-dimensional electromagnetic data generated from a dual-polarized antenna system. The investigation was conducted using a 1,000-sample synthetic dataset containing six electromagnetic features representing electric-field strength, power-flow density, and surface-current density at two orthogonal excitation ports. Through normalization, Euclidean-distance computation, MDS projection, and multidimensional visualization, the study established a systematic approach for converting complex electromagnetic simulation outputs into an interpretable low-dimensional representation.

The quantitative and visual analyses revealed substantial differences between the two excitation ports. In particular, the average power-flow response associated with Port 1 was approximately four times that of Port 2, while the corresponding electric-field and surface-current responses also remained consistently higher at Port 1. These observations demonstrate that the reduced representation was capable of retaining important port-dependent electromagnetic characteristics rather than merely providing a statistical projection. Strong positive associations between electric-field intensity and power flow, together with weaker relationships across the two ports, further indicated the presence of dominant intra-port coupling and partial cross-port decoupling. The MDS stress analysis provided additional evidence for the suitability of a two-dimensional representation. A pronounced decrease in stress occurred when the dimensionality increased from one to two dimensions, after which the improvement became comparatively marginal. This elbow behaviour indicates that the 2D MDS representation provides the most favourable compromise between dimensional simplicity and preservation of the original pairwise structure. The MDS projection also revealed high-density operating regions, localized clusters, energy-distribution gradients, and potential outlying configurations, thereby demonstrating its potential for exploratory antenna diagnostics and anomaly identification.

Overall, the study establishes MDS as a useful quantitative visualization technique for dual-polarized antenna simulation analysis. Its ability to preserve pairwise dissimilarities while reducing a six-dimensional electromagnetic feature space to two dimensions provides engineers with a more accessible representation of complex antenna behaviour. The resulting framework can support early-stage design exploration, excitation-state comparison, clustering, anomaly detection, and feature interpretation. Nevertheless, because the present investigation is based on controlled synthetic simulation data, future studies should validate the framework using experimentally measured antenna data and compare MDS quantitatively with alternative reduction methods such as PCA, t-SNE, UMAP, and autoencoder-based approaches. The current findings therefore provide a reproducible foundation for integrating dimensionality reduction and visual analytics into computational electromagnetic design workflows.

## References


1 Chen, Y., Li, H., and Q. Wu, “Dual-polarized antenna technologies for 5G and beyond: Design, challenges, and future trends,” *IEEE Trans. Antennas Propag.*, vol. *70*, no. 9, pp. 7523–7536, 2022.

2 Quadri Ademola MUMUNI, Adetokunbo Abdul Rasheed ADENOWO, Lateef Adesola AKINYEMI, Oluwagbemiga Omotayo SHOEWU, and Comfort Oluwaseyi FOLORUNSHO. (2022). “Collaborative manufacturing techniques: a review,” Federal University of Oye-Ekiti Journal of Engineering and Technology, Nigeria.vol 7(4), 2579-0625, DOI: https://doi.org/10.46792/fuoyejet.v7i4.891

3 Wang, J. and Y. Huang, “Full-wave electromagnetic solvers for antenna design: A comparative review of CST, HFSS, and FEKO,” *IEEE Antennas Propag. Mag.*, vol. *62*, no. 5, pp. 24–35, 2020. doi: 10.1109/MAP.2020.3012596.

4 Ipinnimo O., Mumuni Q. A., Obayiuwana E., George O.A. (2025).“Analysis of an inductive coupling-based solar-powered wireless charging station,” FUOYE Journal of Innovation Science and Technology.

5 Ahmed, S. and R. Kumar, “Comparative analysis of PCA and nonlinear dimensionality reduction techniques for electromagnetic simulation data,” *IET Microw., Antennas Propag.*, vol. *15*, no. 12, pp. 1450–1461, 2021. doi: 10.1049/mia2.12105.

6 Quadri Ademola Mumuni, Olatayo Moses Olaniyan, Oluwafemi Ipinnimo, Lateef Adesola Akinyemi, and Ameena Idowu Olayiwola-Mumuni. (2025). “Intelligent PID Gain Selection via Supervised Machine Learning Approach for Decoupled MIMO Control Systems,” Journal of Future Artificial Intelligence and Technologies 2025(June), vol. 2, no. 1. DOI : 10.62411/faith.3048-3719-92.

7 Liu, J., Zhang, F., and X. Wang, “Nonlinear dimensionality reduction for electromagnetic simulations: A study of MDS and t-SNE,” *Electronics*, vol. *10*, no. 19, Art. no. 2378, 2021. doi: 10.3390/electronics10192378.

8 Abideen Abiodun YUSSOUFF, Elkanah Olaosebikan OYETUNJI, Nurudeen Adekunle RAJI, Quadri Ademola MUMUNI, “Energy estimation on mini households for development of a mini wind turbine in a low wind energy area. Global Journal of Engineering and Technology Advances, 2023, 15(01), 041–049, DOI: https://doi.org/10.30574/gjeta.2023.15.1.0073

9 Olaniyan, O.M., Bello, K.A., Maladzhi, R.W., Joseph, J.O., Esan, A.O., Mumuni, Q.A., Omodunbi, B.A., & Chiejine, C.M. (2026). A Multi-Instant Machine Learning Algorithm Model for Infant Fingerprinting Verification. Artificial Intelligence and Applications.

10 Huang, X., Wang, T., and Y. Zhao, "Application of multidimensional scaling in antenna array data interpretation," *Prog. Electromagn. Res. C*, vol. *112*, pp. 173–185, 2021. doi: 10.2528/PIERC21042504.

11 Khan, A., Sharma, P., and V. Mehta, "Visualization techniques for high-dimensional antenna simulation data," *Int. J. RF Microw. Comput.-Aided Eng.*, vol. *32*, no. 5, Art. no. e23125, 2022. doi: 10.1002/mmce.23125.

12 Zhang, Y. and X. Liu, "Dimensionality reduction techniques in computational electromagnetics: A survey," *J. Comput. Phys.*, vol. *419*, Art. no. 109677, 2020. doi: 10.1016/j.jcp.2020.109677.

13 Wang, R., Zhou, L., and K. Xu, "Nonlinear data analysis approaches for high-capacity wireless system design," *IEEE Trans. Wireless Commun.*, vol. *21*, no. 7, pp. 5140–5154, 2022. doi: 10.1109/TWC.2022.3164125.

14 Zhang, Y., Wang, H., and P. Zhou, "Principal component analysis-based compression of far-field radiation patterns for efficient antenna analysis," *IEEE Trans. Antennas Propag.*, vol. *69*, no. 11, pp. 7821–7832, 2021. doi: 10.1109/TAP.2021.3089347.

15 Wang, X., Li, Z., and J. Chen, "Linear discriminant analysis for efficient channel modeling in massive MIMO systems," *IEEE Commun. Lett.*, vol. *24*, no. 9, pp. 2019–2023, 2020.

16 Ali, H., Mehmood, A., and S. Riaz, "Visualization of antenna array responses using t-distributed stochastic neighbor embedding (t-SNE)," *IET Microw., Antennas Propag.*, vol. *16*, no. 2, pp. 134–142, 2022.

17 Xu, H., Zhao, T., and M. Liu, "Mutual coupling analysis in phased arrays using uniform manifold approximation and projection (UMAP)," IEEE Trans. Antennas Propag., vol. 71, no. 2, pp. 1553–1565, 2023.

18 Chen, Y., Zhang, L., and H. Wu, "Multi-dimensional scaling-based localization in wireless sensor networks," *Ad Hoc Netw.*, vol. *117*, Art. no. 102475, 2021.

19 Kumar, P., Singh, R., and A. Das, "Multi-dimensional scaling for biological pattern recognition: A case study in genomic clustering," *Pattern Recognit. Lett.*, vol. *158*, pp. 70–78, 2022. doi: 10.1016/j.patrec.2022.04.012.

20 Kim, J. and S. Kang, "Dual-polarized antenna design for beamforming optimization in 5G wireless networks," *IEEE Access*, vol. *9*, pp. 12651–12662, 2021. doi: 10.1109/ACCESS.2021.3051375.

21 Ahmed, I., Hussain, R., and M. Khalid, "Mutual coupling reduction in dual-polarized MIMO systems for 5G applications," *IEEE Trans. Antennas Propag.*, vol. *68*, no. 4, pp. 3121–3132, 2020. doi: 10.1109/TAP.2019.2956789.